ISSN 1023-1935, Russian Journal of Electrochemistry, 2016, Vol. 52, No. 7, pp. 622–627. © Pleiades Publishing, Ltd., 2016.
Original Russian Text © V.A. Kolotygin, A.I. Ivanov, S.I. Bredikhin, V.V. Kharton, 2016, published in Elektrokhimiya, 2016, Vol. 52, No. 7, pp. 697–703.

Electrophysical and Thermomechanical Properties of Perovskites $La_{0.5}A_{0.5}Mn_{0.5}Ti_{0.5}O_{3-\delta}$ (A = Ca, Sr, Ba) Used as Fuel Cell Anodes: the Effect of Radius of Alkali-Earth Cation[1]

V. A. Kolotygin[a], A. I. Ivanov[a, *], S. I. Bredikhin[a], and V. V. Kharton[a, b]

[a] *Institute of Solid State Physics, Russian Academy of Sciences, ul. Akademika Osip'yana 2, Moscow oblast', Chernogolovka, 142432 Russia*

[b] *Center for Research in Ceramics and Composite Materials (CICECO), University of Aveiro, Santiago Campus, 3810-193, Aveiro, Portugal*

**e-mail: aliv@issp.ac.ru*

Received July 15, 2015

Abstract—The effect of the radius of the alkali-earth cation substituted into the *A* sublattice of $La_{0.5}A_{0.5}Mn_{0.5}Ti_{0.5}O_{3-\delta}$ (A = Ca, Sr, Ba) perovskites on their stability and transport and thermomechanical properties is considered. The increase in the cation radius is shown to improve the phase stability and decrease the conductivity under both oxidative and reductive conditions. The thermal and chemical expansion of $La_{0.5}A_{0.5}Mn_{0.5}Ti_{0.5}O_{3-\delta}$ ceramics is studied by dilatometry in controlled atmospheres and a wide temperature range at $p(O_2)=10^{-21}$–0.21 atm. The coefficients of thermal expansion of $La_{0.5}A_{0.5}Mn_{0.5}Ti_{0.5}O_{3-\delta}$ are in the interval of $(10.7–14.3)\times 10^{-6}$ K^{-1}, i.e., compatible with those of standard solid electrolytes of solid-oxide fuel cells. The maximum chemical expansion does not exceed 0.2% at isothermal reduction in the $CO–CO_2$ mixture.

Keywords: conductivity, perovskite, high-temperature dilatometry, chemical expansion, redox stability

DOI: 10.1134/S1023193516070077

INTRODUCTION

At present, perovskite-like solid systems (La, A)(Mn, Ti)$O_{3-\delta}$, where A is an alkali-earth metal cation, are considered as promising materials for anodes, cathodes, and interconnectors of solid-oxide fuel cells (SOFC) [1–13]. It was shown that the presence of manganese in these perovskites provides them the high electrochemical activity, while a sufficient amount of titanium ensures their chemical and thermomechanical stability in a wide range of oxygen partial pressures $p(O_2)$ [1–5, 9–11]. At the same time, the effect of the A cation radius on their functional properties remains practically unknown. These phases are also stable in the presence of hydrocarbon fuels, well resistant to sulfur-containing impurities, and chemically inert with respect to many promising electrolytes and metal current collectors [1, 2, 5, 6, 8, 11–13]. However, one substantial limitation to the use of perovskites (La, A)(Mn,Ti)$O_{3-\delta}$ in practice consists in their insufficient electronic conductivity, especially under reductive conditions, which leads to the increase in the anodic polarization [1–4, 9, 10]. As was shown for perovskite-like ferrites, chromites, manganites, and gallates, the ratio between radii of rare-earth element and alkali-earth metal in the *A* sublattice of perovskite can have a substantial effect on the conductivity and other functional properties of the corresponding materials [13–18]. It was also found that the introduction of a coarser cation Ba^{2+} into the *A* sublattice of the (La, Sr)$TiO_{3-\delta}$ anode improved the electrochemical characteristics of SOFC [19].

The goal of this study was to optimize the composition of (La, A)(Mn,Ti)$O_{3-\delta}$ compounds in order to improve their functional properties. For this purpose, we studied how the radius of the alkali-earth cation-substituent into *A* sublattice of $La_{0.5}A_{0.5}Mn_{0.5}Ti_{0.5}O_{3-\delta}$ (A = Ca, Sr, Ba) perovskites affects their stability in reductive media typical of SOFC anodes, the specific conductivity in oxidative and reductive atmospheres, and the thermal and chemical expansion in a wide range of $p(O_2)$. The ratio of metal cations in the *A* and *B* sublattices of perovskite (50 at %) was chosen for studying being optimal according to the data of [2].

EXPERIMENTAL

The synthesis of polycrystalline materials $La_{0.5}A_{0.5}Mn_{0.5}Ti_{0.5}O_{3-\delta}$ was carried out by the glycine-nitrate method [20] with the use of $La(NO_3)_3 \cdot 6H_2O$, $Ca(NO_3)_2 \cdot 4H_2O$, $Sr(NO_3)_2$, $Ba(NO_3)_2$, $Mn(CH_3COO)_2 \cdot$

[1] Published on the basis of the materials of III All-Russia Conference "Fuel Cells and Power Plants on Their Basis," Chernogolovka, 2015.

Table 1. Unit cell parameters, space groups, and tolerance factors of $La_{0.5}A_{0.5}Mn_{0.5}Ti_{0.5}O_{3-\delta}$ after thermal treatment under oxidative and reductive conditions

Material	Thermal treatment conditions		Tolerance factor*
	air, 1473–1573 K	10–20% H_2–N_2, 973–1223 K	
$La_{0.5}Ca_{0.5}Mn_{0.5}Ti_{0.5}O_{3-\delta}$	*Pbnm* $a = 0.5467(2)$ nm, $b = 0.7754(2)$ nm, $c = 0.5478(2)$ nm	*Pbnm* $a = 0.5497(2)$ nm, $b = 0.7781(2)$ nm, $c = 0.5527(2)$ nm	0.96
$La_{0.5}Sr_{0.5}Mn_{0.5}Ti_{0.5}O_{3-\delta}$	$R\bar{3}c$ $a = 0.5517(2)$ nm, $\alpha = 60.130(3)°$	$R\bar{3}c$ $a = 0.5551(2)$ nm, $\alpha = 60.136(2)°$	0.98
$La_{0.5}Ba_{0.5}Mn_{0.5}Ti_{0.5}O_{3-\delta}$	$Pm\bar{3}m$ $a = 0.3960(2)$ nm	$Pm\bar{3}m$ $a = 0.3964(2)$ nm	1.01

*The tolerance factors were calculated under the assumption of cationic and oxygen stoichiometry, the degrees of oxidation La^{3+}, A^{2+}, Mn^{3+}, and Ti^{4+}, and 12- and 6-fold coordination of A and B cations, respectively.

$4H_2O$, TiO_2, and glycine (grade of purity ⩾99%). Stoichiometric amounts of the corresponding metal salts and glycine were dissolved in distilled water on active stirring until complete homogenization of the medium. Glycine was taken in 1.5-fold mass excess as compared with its stoichiometric amount [20]. Very fine TiO_2 powder was added to the resulting aqueous solution. The suspension was placed on a laboratory electric stove and the reaction of spontaneous combustion was initiated at 473–573 K. The resulting loose deposit was annealed at 1073–1273 K for 2–5 h to remove the decomposition products of metal salts and carbon-containing residues. To provide the complete interaction of TiO_2 with the rest metal oxides, the reaction mixture was repeatedly annealed at 1473–1573 K, which was alternated by its grinding and crushing in a planetary ball mill.

X-ray diffraction patterns were recorded at room temperature on diffractometer Rigaku D/Max-B ($CuK_{\alpha 1}$ radiation, steps of 0.02°, angle range $20° \leqslant 2\theta \leqslant 80°$, with exposure for 1–2 s). The diffraction patterns were processed and the lattice parameters were determined by using programs PowerCell (version 2.4).

The ceramic samples for electrophysical and thermomechanical tests were prepared by the hydraulic uniaxial pressing of single-phase powders (80–100 MPa) followed by sintering at 1723 K for 30 h in air. The specific conductivity was measured by a standard four probe method on direct current with platinum contacts. To improve the sample contact with probes, a layer of platinum paste was placed on the sample surface. The experiments were carried out in air in the flow of 10% H_2–90% N_2 at 563–1273 K. Thermomechanical tests were carried out in a vertical dilatometer Linseis L75/N1 calibrated with respect to a cylindrical Al_2O_3 sample. The tests were carried out in two modes. In the dynamic mode, the sample was permanently heated (3 K/min) up to 1373 K and then cooled (3 K/min) to room temperature. In the thermal cyclic mode, the sample was heated to 1273 K, exposed at this temperature for 2–7 h, and then cooled in the step-wise mode to 973–1223 K with steps of 50 K and isothermal exposure at each temperature until complete equilibration of material with the gas medium. During the measurements, we successively switched the gas flows of air, argon, and the CO–CO_2 mixture prepared by CO_2 reduction by means of an electric pump. Examples of dilatometric curves of equilibration in air and in CO–CO_2 were shown in [2] for $La_{0.5}Sr_{0.5}Mn_{0.5}Ti_{0.5}O_{3-\delta}$. The thermal expansion coefficient (TEC) was determined from the slope of the dependence of relative elongation ($\Delta L/L_0$) of the sample on the temperature. The values of isothermal chemically induced expansion ε at the reduction of material in a given atmosphere as compared with air were calculated based on the equation

$$\varepsilon = \frac{1+\left(\frac{\Delta L}{L_0}\right)_{\text{atm},\,T}}{1+\left(\frac{\Delta L}{L_0}\right)_{\text{air},\,T}} - 1,$$

where $(\Delta L/L_0)_{\text{atm},T}$ and $(\Delta L/L_0)_{\text{air},T}$ correspond to the relative elongation of the sample on its heating from 300 K to a given temperature in a given atmosphere and in air, respectively. The electrochemical pump and the sensor of oxygen pressure were made of a solid electrolyte based on stabilized zirconia with attached platinum electrodes [21].

RESULTS AND DISCUSSION

According to the data of X-ray diffraction analysis, the powders of $La_{0.5}A_{0.5}Mn_{0.5}Ti_{0.5}O_{3-\delta}$ synthesized in air at 1473–1573 K were single-phase with the perovskite-like crystal structure (Fig. 1). An increase in the radius of the alkali-earth cation led to the structural transition ortho rhomb–rhombohedron–cube (Table 1). An important criterion of SOFC anodic materials is their phase stability under oxidative condi-

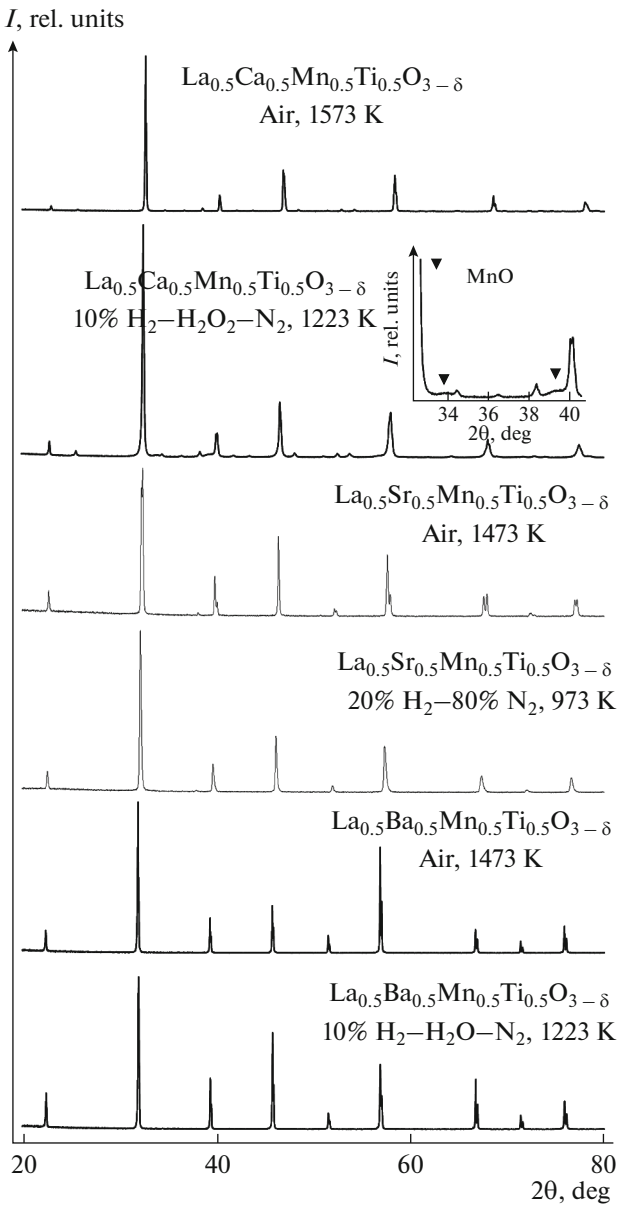

Fig. 1. X-ray powder patterns of $La_{0.5}A_{0.5}Ti_{0.5}Mn_{0.5}O_{3-\delta}$ after annealing in oxidative and reductive atmospheres.

tions (during the synthesis and burning-in of electrode layers) and in the reductive atmosphere of anode operation. To test their resistance to reduction, the $La_{0.5}A_{0.5}Mn_{0.5}Ti_{0.5}O_{3-\delta}$ powders synthesized in air were annealed in a flow of the (10–20%)H_2–N_2 gas mixture at 973–1223 K. For Sr- and Ba-substituted perovskites, the phase composition and the structure remained unchanged, whereas the Ca-substituted material demonstrated the formation of a small amount of admixed MnO (Fig. 1). Under reductive conditions, the partial reduction of Ti^{4+} to Ti^{3+} was observed as well as the reduction of the predominant part of Mn^{4+} ions to the larger Mn^{3+} and Mn^{2+} ions.

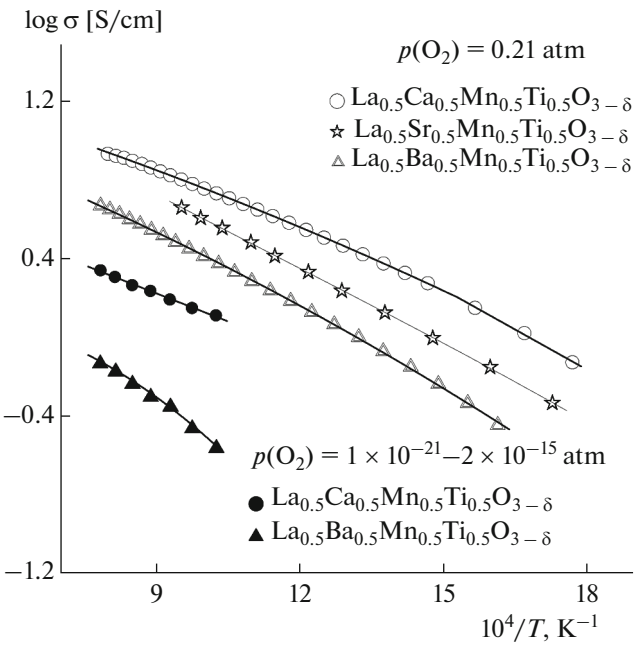

Fig. 2. Temperature dependences of the specific conductivity of $La_{0.5}A_{0.5}Ti_{0.5}Mn_{0.5}O_{3-\delta}$ in air and 10% H_2–N_2 atmosphere.

The content of oxygen which had the constringent effect on the structure decreased. As a result, for $La_{0.5}A_{0.5}Mn_{0.5}Ti_{0.5}O_{3-\delta}$ the lattice parameters were observed to increase (Table 1). The increase in the phase stability under reductive conditions agreed with the Goldschmidt tolerance factors [17] of the corresponding perovskites (Table 1), for instance, for $La_{0.5}Ba_{0.5}Mn_{0.5}Ti_{0.5}O_{3-\delta}$ the tolerance factor slightly exceeded unity and approaching it at the reduction due to the formation of coarse cations Mn^{2+} and Ti^{3+}.

Figure 2 shows the temperature dependences of the specific conductivity of $La_{0.5}A_{0.5}Mn_{0.5}Ti_{0.5}O_{3-\delta}$ ceramic samples in oxidative and reductive atmospheres. Conductivity is thermally activated and well described within the framework of the standard model of Arrhenius; the activation energy (E_a) is in the interval of 26.5–34.8 kJ/mol (Table 2). The specific conductivity and E_a of $La_{0.5}A_{0.5}Mn_{0.5}Ti_{0.5}O_{3-\delta}$ are comparable with those of certain alternative SOFC anodes based on (La, A)(Mn, Cr)$O_{3-\delta}$ with the similar crystal structure and the close content of manganese [14, 15]. The $La_{0.5}Ca_{0.5}Mn_{0.5}Ti_{0.5}O_{3-\delta}$ composite exhibited the highest conductivity under all conditions. The increase in the radius of the alkali-earth cation in *A* sublattice induced a decrease in conductivity under both oxidative and reductive conditions and also an increase in the corresponding activation energy (Figs. 2, 3). This tendency is explained by the increase in the A–O bond length with the increase in the A^{2+} radius, which results in a decrease in the degree of overlap of 3*d* orbitals of manganese atoms with

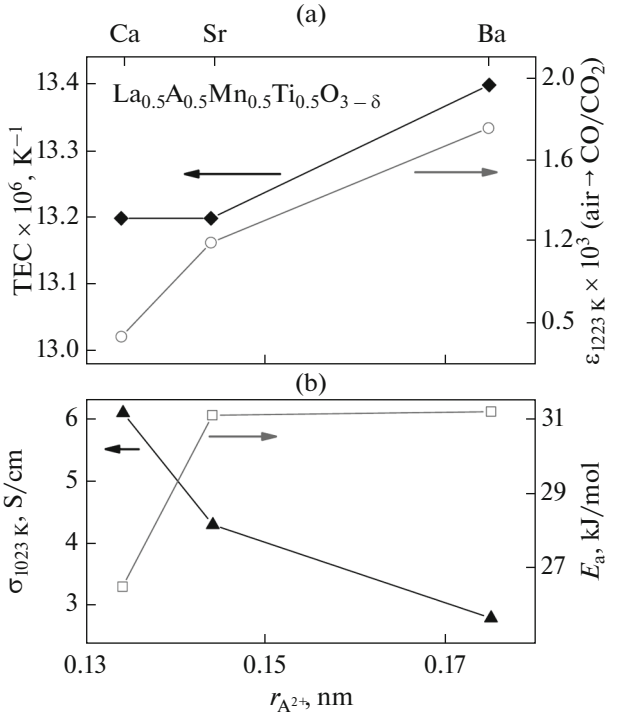

Fig. 3. Specific conductivity, activation energy of conduction in air, and coefficients of thermal and chemical expansion for $La_{0.5}A_{0.5}Ti_{0.5}Mn_{0.5}O_{3-\delta}$ as a function of the radius of alkali-earth cation-substituent in A sublattice.

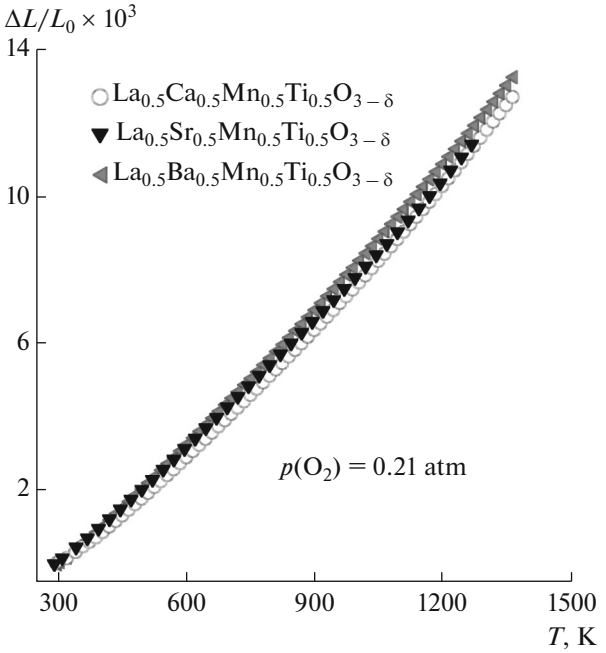

Fig. 4. Dilatometric curves for $La_{0.5}A_{0.5}Ti_{0.5}Mn_{0.5}O_{3-\delta}$ ceramics measured in the mode of permanent heating in air (3 K/min); L_0 corresponds to the original length at room temperature.

2*p* orbitals of oxygen atoms. The lowest conductivity observed for $La_{0.5}Ba_{0.5}Mn_{0.5}Ti_{0.5}O_{3-\delta}$ can be associated also with formation of local microdeformations of the perovskite lattice due to the great difference between sizes of cations La^{3+} ($r_{La^{3+}}$ = 0.136 nm) and Ba^{2+} ($r_{Ba^{3+}}$ = 0.161 nm), which results in scattering of charge carriers [14–16]. The conductivity of materials under reductive conditions substantially decreased (Fig. 2), which was associated with the decrease in the concentration of charge carriers of the *p* type due to reduction of $Mn^{4+}$to Mn^{2+}/Mn^{3+} [1–3].

Figures 3–5 and Tables 3 and 4 show the results of dilatometric measurements carried out on $La_{0.5}A_{0.5}Mn_{0.5}Ti_{0.5}O_{3-\delta}$ ceramics under different conditions. Within instrumental error, the TEC of $La_{0.5}Sr_{0.5}Mn_{0.5}Ti_{0.5}O_{3-\delta}$ in air (13.0± 0.1)× 10^{-6} K^{-1} coincided with that found in [9]. The TEC of $La_{0.5}A_{0.5}Mn_{0.5}Ti_{0.5}O_{3-\delta}$ varied in the interval of (10.7–14.3) × 10^{-6} K^{-1} (Table 3) typical of perovskite-like manganites and titanates and also of materials of standard electrolytes [18, 22]. As the temperature increased, the apparent TEC also increased as a result of the exit of oxygen from the perovskite lattice (Fig. 4, Table 3). The TEC values were virtually independent of $p(O_2)$ under oxidative conditions ($p(O_2)$ = 10^{-4}–0.21 atm) and increased insignificantly with the transition to the reductive atmosphere, which

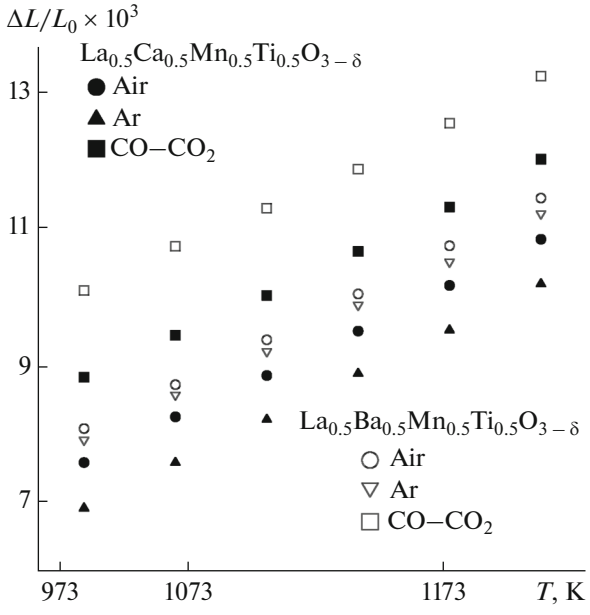

Fig. 5. Relative elongation of $La_{0.5}A_{0.5}Ti_{0.5}Mn_{0.5}O_{3-\delta}$ ceramics in different atmospheres.

Table 2. Activation energies of specific conductivity of $La_{0.5}A_{0.5}Mn_{0.5}Ti_{0.5}O_{3-\delta}$ materials in air

Material	Temperature interval, K	Activation energy, kJ/mol
$La_{0.5}Ca_{0.5}Mn_{0.5}Ti_{0.5}O_{3-\delta}$	683–1253	26.5 ± 0.1
	563–683	29.8 ± 3.8
$La_{0.5}Sr_{0.5}Mn_{0.5}Ti_{0.5}O_{3-\delta}$	473–1053	30.3 ± 0.2
$La_{0.5}Ba_{0.5}Mn_{0.5}Ti_{0.5}O_{3-\delta}$	753–1273	31.9 ± 0.1
	613–753	34.8 ± 1.7

also agreed with relationships observed for the chemical expansion (Fig. 5, Table 4). As in the case of (La, Sr)(Mn, Cr, Ti)$O_{3-\delta}$ and (La, Sr)(Mn, Ti)$O_{3-\delta}$, the isothermal expansion of $La_{0.5}A_{0.5}Mn_{0.5}Ti_{0.5}O_{3-\delta}$ was associated with the decrease in the average degree of oxidation and, correspondingly, the increase in the ionic radius of cations in *B* sublattice of perovskite [2, 3]. Due to the tendency towards wider changes in the oxygen stoichiometry and the increase in lattice microdeformations [14–16], the level of thermal and chemical expansion increased in the series $La_{0.5}Ca_{0.5}Mn_{0.5}Ti_{0.5}O_{3-\delta} < La_{0.5}Sr_{0.5}Mn_{0.5}Ti_{0.5}O_{3-\delta} < La_{0.5}Ba_{0.5}Mn_{0.5}Ti_{0.5}O_{3-\delta}$ (Figs. 3–5). However, for the material with the maximum volume variations, $La_{0.5}Ba_{0.5}Mn_{0.5}Ti_{0.5}O_{3-\delta}$, the TEC values under oxidative and reductive conditions were 13.3×10^{-6} K^{-1} and 12.4×10^{-6} K^{-1}, respectively (Table 3) and the level of its chemical expansion at the reduction did not

Table 3. Thermal expansion coefficients of $La_{0.5}A_{0.5}Mn_{0.5}Ti_{0.5}O_{3-\delta}$ ceramics at different $p(O_2)$

Material	$p(O_2)$, atm	T, K	TEC × 10^6, K^{-1}
$La_{0.5}Ca_{0.5}Mn_{0.5}Ti_{0.5}O_{3-\delta}$	0.21	303–923	10.7 ± 0.1
		923–1223	13.0 ± 0.1
		1223–1373	14.0 ± 0.1
	1×10^{-4}	973–1223	13.1 ± 0.2
	1×10^{-21}–2×10^{-15}	973–1223	12.7 ± 0.5
$La_{0.5}Sr_{0.5}Mn_{0.5}Ti_{0.5}O_{3-\delta}$	0.21	303–923	11.2 ± 0.1
		923–1223	12.8 ± 0.1
	1×10^{-4}	923–1273	12.9 ± 0.1
	3×10^{-20}–2×10^{-11}	923–1273	13.4 ± 0.2
$La_{0.5}Ba_{0.5}Mn_{0.5}Ti_{0.5}O_{3-\delta}$	0.21	303–923	11.4 ± 0.1
		923–1223	13.3 ± 0.1
		1223–1373	14.3 ± 0.1
	1×10^{-4}	973–1223	13.3 ± 0.3
	1×10^{-21}–2×10^{-15}	973–1223	12.4 ± 0.7

Table 4. Relative change in the length of $La_{0.5}A_{0.5}Mn_{0.5}Ti_{0.5}O_{3-\delta}$ ceramics on isothermal reduction (up to $p(O_2) = 10^{-11}$–10^{-21} atm)

T, K	$(L-L_{air})/L_{air} \times 10^3$		
	$La_{0.5}Ca_{0.5}Mn_{0.5}Ti_{0.5}O_{3-\delta}$	$La_{0.5}Sr_{0.5}Mn_{0.5}Ti_{0.5}O_{3-\delta}$	$La_{0.5}Ba_{0.5}Mn_{0.5}Ti_{0.5}O_{3-\delta}$
1223	0.74	1.20	1.76
1173	0.72	1.18	1.77
1123	0.73	1.14	1.80
1073	0.74	1.09	1.90
1023	0.76	1.07	2.00
973	0.82	1.07	2.00

exceed 0.2% (Table 4), which makes this group of materials suitable for using as SOFC electrodes.

CONCLUSIONS

Solid solutions with the perovskite-like structure $La_{0.5}A_{0.5}Mn_{0.5}Ti_{0.5}O_{3-\delta}$ (A = Ca, Sr, Ba) were synthesized. The increase in the radius of the alkali-earth metal-substituent was shown to result in the orthorhomb–rhombohedron–cube structural transition. For the Ba-substituted perovskite, the closeness of the tolerance factor to 1 was shown to provide the high stability of the cubic perovskite phase in a wide interval of $p(O_2)$, whereas the orthorhombic perovskite $La_{0.5}Ca_{0.5}Mn_{0.5}Ti_{0.5}O_{3-\delta}$ with the tolerance factor 0.96 tended to decompose on reduction to form a phase with admixed MnO. The conductivity of oxides was shown to lower down with the increase in the radius of the cation-dopant under both oxidative and reductive conditions. High-temperature dilatometric measurements in controlled atmospheres served for studying the thermal and chemical expansion of $La_{0.5}A_{0.5}Mn_{0.5}Ti_{0.5}O_{3-\delta}$ ceramics at $p(O_2) = 10^{-21}$–0.21 atm. The coefficients of thermal expansion of $La_{0.5}A_{0.5}Mn_{0.5}Ti_{0.5}O_{3-\delta}$ were close to values typical of standard solid electrolytes being in the interval of $(10.7–14.3) \times 10^{-6}$ K^{-1}. The level of thermal and chemical expansion increased in the row Ca < Sr < Ba due to strengthening of the tendency towards the formation of oxygen vacancies and the increase in lattice microdeformations.

ACKNOWLEDGEMENTS

This study was carried out with the financial support by the Ministry of Education and Science of the Russian Federation (contract no. 14.V25.31.0018) and the Russian Foundation for Basic Research (grant no. 13-03-12409).

REFERENCES

1. Ivanov, A.I., Agarkov, D.A., Burmistrov, I.N., Kudrenko, E.A., Bredikhin, S.I., and Kharton, V.V., *Russ. J. Electrochem.,* 2014, vol. 50, p. 730.
2. Kolotygin, V.A., Tsipis, E.V., Ivanov, A.I., Fedotov, Y.A., Burmistrov, I.N., Agarkov, D.A., Sinitsyn, V.V., Bredikhin, S.I., and Kharton, V.V., *J. Solid-State Electrochem.,* 2012, vol. 16, p. 2335.
3. Kolotygin, V.A., Tsipis, E.V., Shaula, A.L., Naumovich, E.N., Frade, J.R., Bredikhin, S.I., and Kharton, V.V., *J. Solid-State Electrochem.,* 2011, vol. 15, p. 313.
4. Kolotygin, V.A., Tsipis, E.V., Lu, M.F., Pivak, Y.V., Yarmolenko, S.N., Bredikhin, S.I., and Kharton, V.V., *Solid State Ionics,* 2013, vol. 251, p. 28.
5. Zhou, X., Yan, N., Chuang, K.T., and Luo, J., *RSC Adv.,* 2014, vol. 4, p. 118.
6. Ovalle, A., Ruiz-Morales, J.C., Canales-Vazquez, J., Marrero-Lopez, D., and Irvine, J.T.S., *Solid State Ionics,* 2006, vol. 177, p. 1997.
7. Escudero, M.J., Irvine, J.T.S., and Daza, L., *J. Power Sources,* 2009, vol. 192, p. 43.
8. Yoon, J.S., Lim, Y.-S., Choi, B.H., and Hwang, H.J., *Int. J. Hydrogen Energy,* 2014, vol. 39, p. 7955.
9. Martinez-Coronado, R., Alonso, J.A., Aguadero, A., Perez-Coll, D., and Fernandez-Diaz, M.T., *J. Appl. Phys.,* 2013, vol. 113, p. 123708.
10. Fu, Q.X., Tietz, F., and Stover, D., *J. Electrochem. Soc.,* 2006, vol. 153, p. D74.
11. Hosseini, N.R., Sammes, N.M., and Chung, J.Sh., *J. Power Sources,* 2014, vol. 245, p. 599.
12. Kim, J.H., Miller, D., Schlegl, H., McGrouther, D., and Irvine, J.T.S., *Chem. Mater.,* 2011, vol. 23, p. 3841.
13. Kim, J.H., Schlegl, H., and Irvine, J.T.S., *Int. J. Hydrogen Energy,* 2012, vol. 37, p. 14511.
14. Jiang, S.P., Li, L., Ong, Kh.P., Wu, P., Li, J., and Jian Pu, J., *J. Power Sources,* 2008, vol. 176, p. 82.
15. Zhang, L., Chen, X., Jiang, S.P., He, H.Q., and Xiang, Ya., *Solid State Ionics,* 2009, vol. 180, p. 1076.
16. Kharton, V.V., Kovalevsky, A.V., Patrakeev, M.V., Tsipis, E.V., Viskup, A.P., Kolotygin, V.V., Yaremchenko, A.A., Shaula, A.L., Kiselev, E.A., and Waerenborgh, J.C., *Chem. Mater.,* 2008, vol. 20, p. 6457.
17. Hayashi, H., Inaba, H., Matsuyama, M., Lan, N.G., Dokiya, M., and Tagawa, H., *Solid State Ionics,* 1999, vol. 122, p. 1.
18. Tsipis, E.V. and Kharton, V.V., *J. Solid-State Electrochem.,* 2008, vol. 12, p. 1367.
19. Vincent, A., Luo, J.-L., Chuang, K.T., and Sanger, A.R., *J. Power Sources,* 2010, vol. 195, p. 769.
20. Patil, K.C., Hegde, M.S., Rattan, T., and Aruna, S.T., *Chemistry of Nanocrystalline Oxide Materials: Combustion Synthesis, Properties and Applications*, New Jersey: World Scientific, 2008.
21. Kharton, V.V., *Solid State Electrochemistry I: Fundamentals, Materials and their Applications,* Weinheim: Wiley-VCH, 2009.
22. Tsipis, E.V. and Kharton, V.V., *J. Solid-State Electrochem.,* 2008, vol. 12, p. 1039.

Translated by T. Ya. Safonova